

To be or not to be Asymmetric? VLTI/MIDI and the Mass-loss Geometry of AGB Stars

Claudia Paladini¹
 Daniela Klotz²
 Stephane Sacuto^{2,3}
 Eric Lagadec⁴
 Markus Wittkowski⁵
 Andrea Richichi⁶
 Josef Hron²
 Alain Jorissen¹
 Martin A. T. Groenewegen⁷
 Franz Kerschbaum²
 Tijn Verhoelst⁸
 Gioia Rau²
 Hans Olofsson⁹
 Ronny Zhao-Geisler¹⁰
 Alexis Matter⁴

¹ Institut d'Astronomie et d'Astrophysique, Université libre de Bruxelles, Belgium

² Department of Astrophysics, University of Vienna, Austria

³ Department of Physics and Astronomy, Division of Astronomy and Space Physics, University of Uppsala, Sweden

⁴ Laboratoire Lagrange, Université Côte d'Azur, Observatoire de la Côte d'Azur, CNRS, Nice, France

⁵ ESO

⁶ National Astronomical Research Institute of Thailand, Chiang Mai, Thailand

⁷ Koninklijke Sterrenwacht van België, Brussel, Belgium

⁸ Belgian Institute for Space Aeronomy, Brussels, Belgium

⁹ Department of Earth and Space Sciences, Onsala Space Observatory, Sweden

¹⁰ Department of Earth Sciences, National Taiwan Normal University, Taipei, Taiwan

The Mid-infrared Interferometric instrument (MIDI) at the Very Large Telescope Interferometer (VLTI) has been used to spatially resolve the dust-forming region of 14 asymptotic giant branch (AGB) stars with different chemistry (O-rich and C-rich) and variability types (Miras, semi-regular, and irregular variables). The main goal of the programme was to detect deviations from spherical symmetry in the dust-forming region of these stars. All the stars of the sample are well resolved with the VLTI, and five are asymmetric and O-rich. This finding contrasts with observations in the near-infrared, where the C-rich objects are found to be more asymmetric than the

O-rich ones. The nature of the asymmetric structures so far detected (dusty discs versus blobs) remains uncertain and will require imaging on milli-arcsecond scales.

Background

Stars with low to intermediate initial mass ($\leq 8 M_{\odot}$), including our Sun, undergo a short evolutionary phase, called the AGB, towards the end of their lives and undergo several mass dredge-up events. Stars on the AGB usually have O-rich chemistry. However, after the third dredge-up, stars with initial masses between 1 and $4 M_{\odot}$ can reach a C/O ratio > 1 , and their spectra are then dominated by C-bearing molecular and dust species.

The atmosphere of a star on the AGB can be as large as a few au, and it is stripped away by a stellar wind on a typical time-scale of thousands of years. Observations of the following evolutionary stages, the post-AGB and planetary nebula, show some very asymmetric envelopes and emission nebulae around the central star. For many years, AGB stellar mass loss was considered to be mainly symmetric. It is accepted in the planetary nebula community that binary interaction can be responsible for the asymmetric morphology (Jones & Boffin, 2017), but the population of binaries on the AGB does not match that in the post-AGB phase. In fact, because of the pulsation of the star itself and the dust around the AGB star, the companions are difficult to detect.

Between 2009 and 2013, the Herschel Space Telescope imaged the interface between the outer atmosphere and the interstellar medium for a sample of AGB stars within the MESS (Mass-loss from Evolved StarS) guaranteed observing time programme (Groenewegen et al., 2011). The MESS programme identified four different geometries: ring, fermata, eye and irregular (Cox et al., 2012). The ring shape is due to the interaction between different episodic mass-loss events; the fermata (so named because of its similarity to the symbol used in music) is caused by interaction between the stellar wind and the interstellar medium; the eye shape is due to a mixture of the previous two mechanisms, and possibly the

interaction with an unseen companion; and the irregular shape applies to objects showing extended and non-detached material (as opposed to rings).

Observations carried out using other techniques (from near-infrared interferometric campaigns to radio and sub-millimetre studies — examples include: Cruzalèbes et al., 2015; Lykou et al., 2015; Kervella et al., 2014; Ramstedt et al., 2014; and Maercker et al., 2012) showed a very complex picture. Altogether it became clear that observations needed to probe all spatial scales for a defined sample of stars in order to understand the physics of the outflow.

The VLTI/MIDI survey

Our VLTI/MIDI Large Programme (Paladini et al., 2017) observed a subsample of the MESS targets to understand how asymmetric structures develop within a very few stellar radii ($2\text{--}10 R_{\star}$) of the atmosphere as a result of the mass-loss process. The questions we wanted to answer were: (i) whether the mass loss is an episodic process; (ii) where the asymmetric structures form, and what is the mechanism responsible; (iii) how do the asymmetries change as the star moves up the AGB; and (iv) whether the asymmetric structures detected by Herschel are connected to the ones eventually observed in the inner atmospheres of AGB stars.

Of course, performing a study of the global geometry with a two-telescope beam combiner is very challenging. However, MIDI was the only facility available worldwide with the angular resolution needed to resolve the inner dust-forming region of these stars. We carried out an extensive preparatory study to select the right baselines to sample the same spatial frequencies in all targets necessary for simple morphology studies. For this we used the Jean-Marie Mariotti Centre (JMMC) tool Aspro2¹ and the ESO Vis-Calc² tool. An in-house tool optimised for MIDI was also developed to analyse the data (GEometrical Model Fitting for INterferometric Data [GEM-FIND]; Klotz et al., 2012).

A total of 115 hours on the Auxiliary Telescopes was devoted to observing the

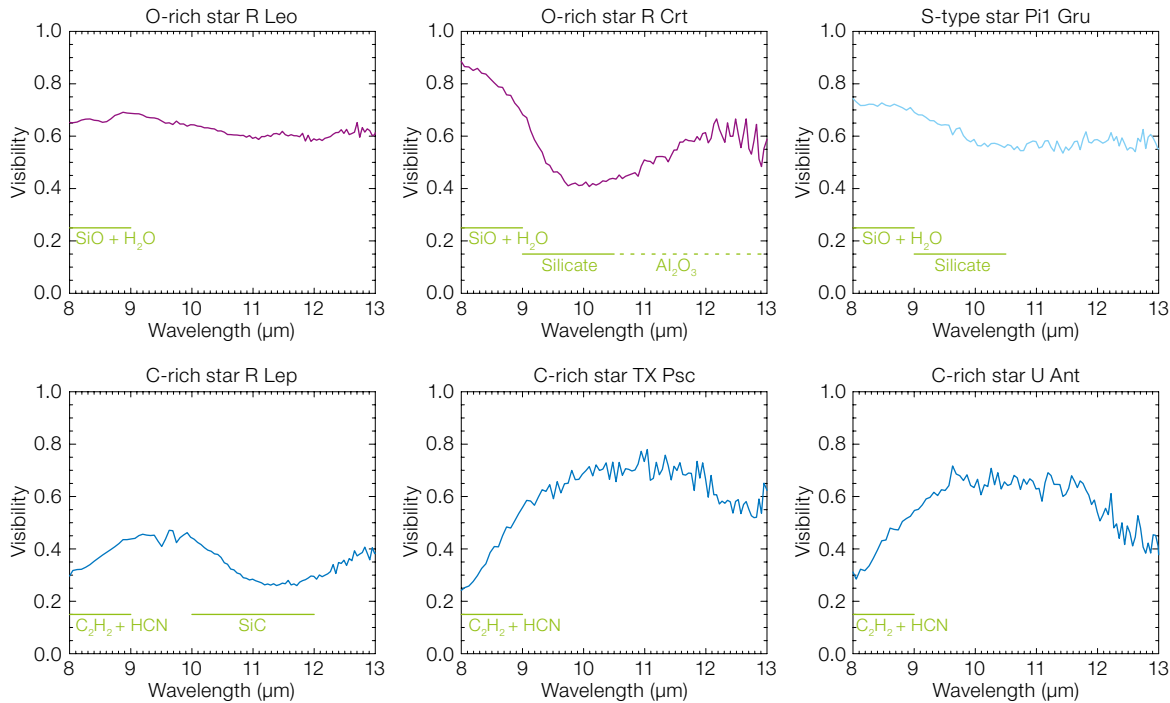


Figure 1. Some examples of the MIDI visibility spectra of AGB stars with different chemistry observed within the programme. The molecular and dust features characterising the visibility spectra are highlighted. The typical error bar is of the order of 10%. From Paladini et al. (2017).

14 targets initially selected. The objects have different chemistry: five are O-rich stars with $C/O < 1$; two are S-type stars with $0.5 < C/O < 1$; and seven are C-rich stars with $C/O > 1$. When available for any of the selected targets, archival data were also analysed.

Visibility versus wavelength

The MIDI observables are photometry, visibility amplitudes and differential phases spread across the *N*-band (8–13 μm). The analysis of the visibilities (also called the visibility spectrum) provides information about the brightness and angular size of the molecular and dust components of the envelope. Figure 1 shows the typical visibility spectra of the O-rich cases (upper row), where SiO and water molecules dominate the region between 8 and 9 μm . Silicate dust emission in the integrated spectrum usually corresponds to a drop in the visibility around 10 μm . Such a visibility drop indicates that the envelope is more extended and/or brighter in that wavelength range.

The C-rich counterparts of the sample (examples in the lower row in Figure 1) have different visibility spectrum morphology. A drop in the visibility between 8 and

9 μm , where C_2H_2 and HCN molecules contribute, is observed for all the C-stars. Evolved Mira variables, such as R Lep, show a drop in the visibility around 11 μm , where the SiC dust feature appears. Stars without SiC emission in the integrated spectrum have a visibility more like that of TX Psc (Figure 1, lower row, central panel).

Peculiar cases

In the literature to date, all the features identified in the mid-infrared spectra of AGB stars have always been mirrored in the visibility spectrum. However, we observed two interesting and unexpected cases in our sample. The Infra-Red Astronomical Satellite (IRAS) and MIDI spectra of the C-rich star U Ant show the typical 11.3 μm silicon carbide dust feature, but there is no trace of such a feature in the visibility spectrum (Figure 1, lower row, right panel). It might therefore be that the interferometer is resolving out the dust shell in this case.

Another peculiar star in our sample is the C-star S Sct. While SiC dust is clearly detected in the Infrared Space Observatory (ISO) spectrum, there is no trace of such a feature in the MIDI spectrum and

in the visibility. Perhaps a recent episodic strong stellar wind might have dissolved the shell, but no such event has been reported in the literature.

Follow-up observations with the VLT Imager and Spectrometer for mid-InfraRed (VISIR) and the VLTI second-generation instrument Multi AperTure mid-Infrared SpectroScopic Experiment (MATISSE), see Lopez et al. (2006) and Kasper et al. (2013), as well as detailed dynamic modeling (for example, Rau et al., 2017), should help to solve the mystery of these two stars.

Variability

The rich archive of MIDI observations gave us the chance to study the interferometric and spectroscopic variability for some targets. Comparing visibility spectra taken at different visual phases, but with the same projected baseline and position angle, gives information on the size variation of the target. On the other hand, the variability in the integrated spectra corresponds to variation in the colour (temperature).

The only case of interferometric variability detected in our sample is shown in

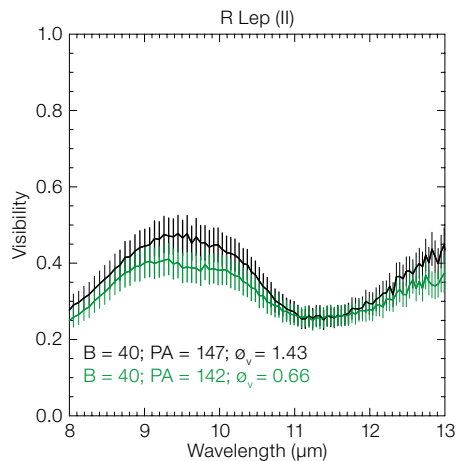


Figure 2. Interferometric variability for the C-rich Mira star R Lep. Comparison between two visibility spectra observed at different visual phases, with the same position angle and projected baseline, is shown.

Figure 2. The observations of the C-rich Mira star R Lep indicate that the molecular environment (8–10 μm) is slightly smaller before minimum visual phase (green line). No size variation is observed, however, in the SiC dust emission wavelength region (~ 11 μm).

These findings confirm that interferometric variability is connected to pulsation, as previously reported by Ohnaka et al. (2007) for V Oph.

We observed flux variation within photometric cycles for four targets. In all the cases the *N*-band magnitude variation is of the order of 0.8–1 mag. For the semi-

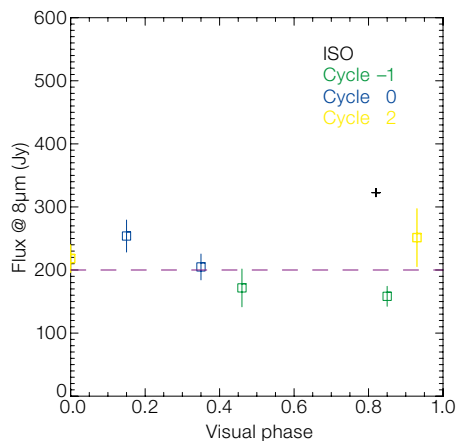


Figure 3. Spectroscopic variability observed with MIDI over several cycles for the O-rich semiregular variable RT Vir. From Paladini et al. (2017).

regular variable RT Vir, the fluxes observed with MIDI at different visual phases follow a sinusoid where the *N*-band maximum is slightly shifted with respect to the visual maximum (Figure 3). These findings agree with previous work (Le Bertre, 1993; Karoricova et al., 2011, and references therein).

Morphology

The main goal of our investigation was to study the geometry of the targets, with a focus on the detection of non-spherical symmetry. A model-independent way to achieve this goal consists in comparing visibilities probing the same spatial frequency at different position angles. A second approach is to use the differential phase observed; objects with a spherical brightness distribution have differential phases equal to zero or 180 degrees. Alongside these two direct methods, we tested the data with spherical, elliptical, and two-component geometrical models.

The differential phase of the two O-rich stars, RT Vir and R Leo, immediately indicates that the stellar environment of these stars is very complex. The analysis of the other objects showed that all the carbon stars were surprisingly symmetric. Both the S-type objects are asymmetric, as is one of the remaining O-rich stars. In summary, we find that asymmetric structures in the *N*-band wavelength domain are more common among the stars with O-rich chemistry.

This result is illustrated in Figure 4 on an IRAS colour-colour diagram.

Near-infrared observations point to the fact that carbon stars are very asymmetric and O-rich objects are not; thermal infrared data show that the percentage of asymmetries between AGB stars with different chemistry is nearly the same (Blasius et al., 2012). This result can be interpreted in terms of the dust composition and characteristics of the stars with different chemistry. The O-rich dust in the near-infrared is nearly transparent, as one sees deeper into the envelope, and not as many asymmetries are expected in that wavelength range. On the other hand, the C-rich dust absorbs the radiation in the near-infrared, making the stars appear blob-like. In the mid-infrared, the O-rich dust is more blobby than in the C-rich cases because there are stronger non-linear effects in the radiative acceleration.

Prospects

Our Large Programme has shown that the stellar wind produces asymmetric structures in the very inner part of the dust-forming region. However, the nature of such asymmetries (dust clumps versus circumstellar discs) will require an imaging campaign with MATISSE. Our programme initially included a VISIR campaign, designed to fill in the gap between the spatial scales of MIDI and Herschel (see Figure 5 for the colour-colour plot of

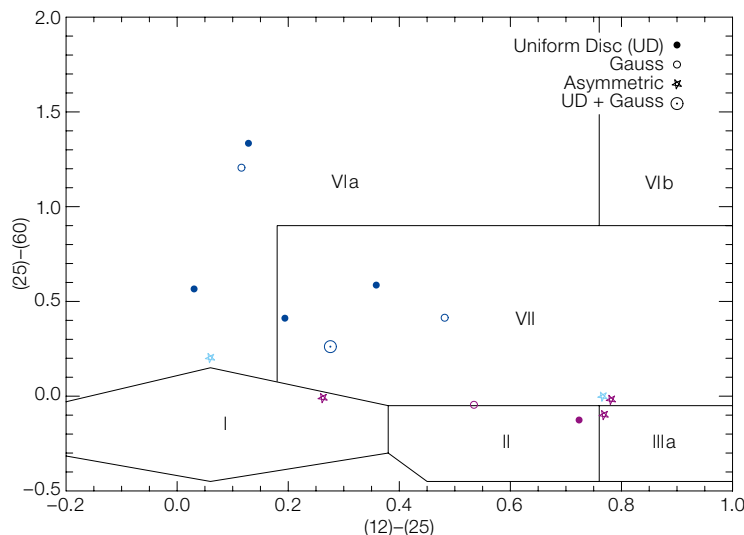


Figure 4. The targets analysed in the programme plotted in the IRAS colour-colour diagram (van der Veen & Habing, 1988). The lower part of the diagram is populated with O-rich stars (magenta) and S-type stars (bright blue). The C-rich objects are located in boxes VIa and VII. Asymmetric targets (stars) are concentrated in the lower part of the diagram.

object morphology). However, adverse weather conditions, and the decommissioning of VISIR for upgrade, prevented us from carrying out this part of the programme. Future observations in this direction are planned.

Acknowledgements

This work was supported by the Austrian Science Fund FWF under the project AP23006, the Belgian Federal Science Policy Office via the PRODEX Programme of ESA, the Belgian Fund for Scientific Research F.R.S.- FNRS, and the European Union's Seventh Framework Programme under Grant Agreement 312430. This research has made use of the SIMBAD database, operated at CDS Strasbourg, France. We acknowledge with thanks the variable star observations from the AAVSO International Database contributed by observers worldwide and used in this research. We thank the ESO Paranal team for supporting our VLT/MIDI observations. F. Bufano, L. Burtscher, M. Cesetti, S. Höfner, T. Lebzelter, J.-B. Le Bouquin, G. C. Sloan, and K. Tristram are thanked for their key contributions.

References

Blasius, T. D. et al. 2012, MNRAS, 426, 4
 Cox, N. L. J. et al. 2012, A&A, 537, A35
 Cruzalèbes, P. et al. 2015, A&A, 446, 3277
 Groenwegen, M. A. T. et al. 2011, A&A, 526, A162

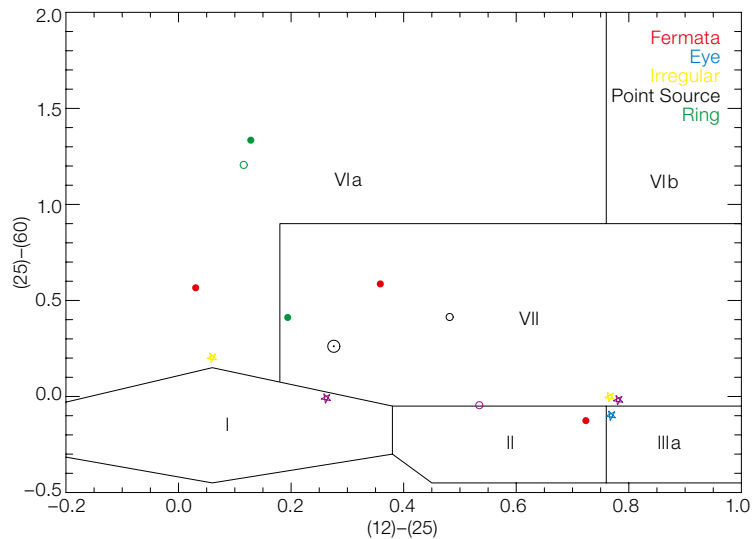


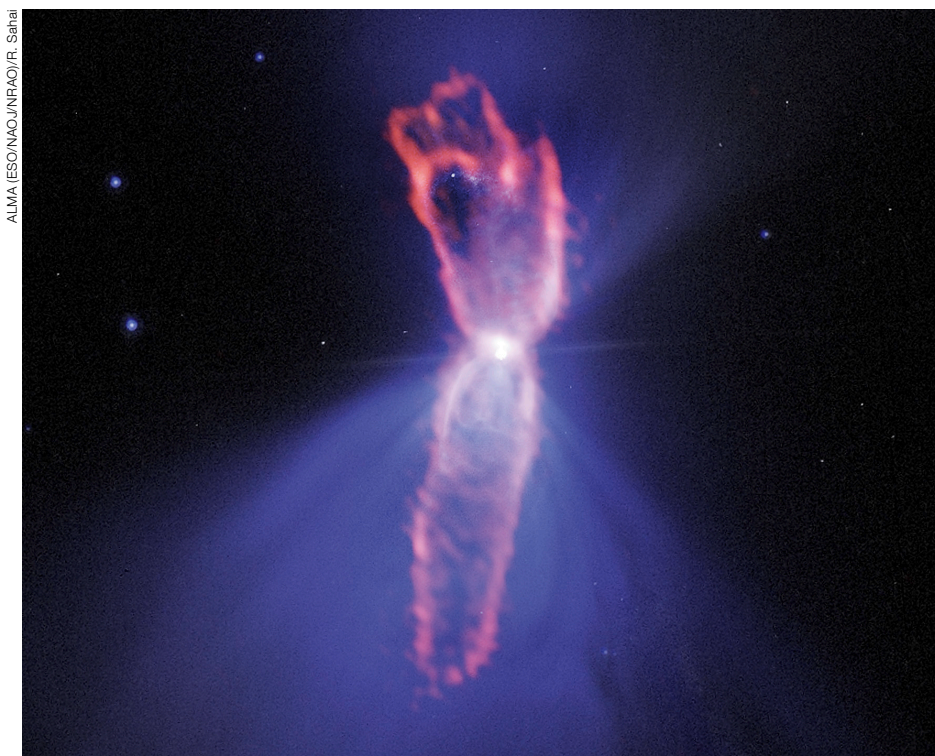
Figure 5. Same as Figure 4 (van der Veen & Habing, 1988) but colour-coded by the Herschel morphology identified in Cox et al. (2012). Linking the Herschel and MIDI observations will require the intermediate spatial scales probed by VISIR.

Jones, D. & Boffin, H. 2017, NatAs, 1, 117
 Karovicova, I. et al. 2011, A&A, 532, A134
 Kervella, P. et al. 2014, A&A, 564, 88
 Klotz, D. et al. 2012, Proc. SPIE, 8445, 84451
 Le Bertre, T. 1993, A&AS, 97, 729
 Lykou, F. et al. 2015, A&A, 576, 46
 Lopez, B. et al. 2006, Proc. SPIE, 6268, 62680
 Maercker, M. et al. 2012, Nature, 490, 212
 Ohnaka, K. et al. 2007, A&A, 484, 371
 Paladini, C. et al. 2017, A&A, 600, 136
 Ramstedt, S. et al. 2014, A&A, 570, 14

Rau, G. et al. 2017, A&A, 600, 92
 van der Veen, W. E. C. J. & Habing, H. J. 1988, A&A, 194, 125

Links

¹ JMMC interferometric tool Aspro2: http://www.jmmc.fr/aspro_page.htm
² ESO VisCalc tool: <https://www.eso.org/observing/etc/>



Composite Atacama Millimeter/submillimeter Array (ALMA) and NASA/ESA Hubble Space Telescope (HST) image of the pre-planetary nebula, the Boomerang, which was ejected by an evolved low mass star. The background bipolar structure (purple) is from the HST visible light image, while the narrow elongated CO (3-2) emission mapped by ALMA is shown in orange. The outflow has exceptionally low brightness temperature (≤ 10 K). See Picture of the Week potw1724 for more details.